

EXPLORATION OF LINOLEIC ACID AS A POTENTIAL THERAPEUTIC AGENT IN ALCOHOLIC LIVER DISEASE VIA NETWORK PHARMACOLOGY AND MOLECULAR SIMULATIONS

Apeksha Rathi¹, Ekta Bhatt¹, Chakresh Kumar Jain^{1*}

¹Department of Biotechnology, Jaypee Institute of Information technology, A-10, Sector-62, Noida-201309, U.P., India,

*Corresponding authors' email: chakresh.jain@mail.jiit.ac.in

ABSTRACT

Linoleic acid, an omega-6 polyunsaturated fatty acid, has been associated with several biological activities, although its therapeutic mechanisms are not fully understood. This study investigated its potential role in Alcoholic Liver Disease (ALD) using an integrated computational approach involving network pharmacology, molecular docking, and molecular dynamics (MD) simulations. The structure of linoleic acid was obtained from PubChem, and pharmacokinetic properties were assessed using TCMSP. Potential targets were identified via CTD, followed by Gene Ontology and KEGG pathway enrichment analysis using WebGestalt. Protein-protein interaction networks were constructed using STRING and visualized in Cytoscape. A total of 38 targets were identified, with strong interconnections suggesting coordinated biological roles. Pathway analysis indicated involvement in key ALD-related processes. Docking studies showed favorable binding affinities of linoleic acid with major target proteins. A 500 ns MD simulation of the linoleic acid-2ZNN complex demonstrated structural stability, supported by RMSD, radius of gyration, SASA, PCA, and MM/PBSA analyses. Overall, linoleic acid may exert therapeutic effects in ALD through multi-target mechanisms. While limitations such as low bioavailability exist, the findings provide a basis for further experimental validation.

KEYWORDS: Linoleic acid, Alcoholic liver disease, genes, molecular docking, Bioinformatic analysis

INTRODUCTION

Alcoholic liver disease (ALD) is rapidly increasing universally, which is raising the number of deaths and increasing the overall healthcare costs[1]. Increasing consumption of alcohol and misuse strains public health resources in addition to having a detrimental effect on individual health[2]. This study helps in knowing the bioactive compound Linoleic acid and how it can reduce the Alcoholic liver diseases if consumed in right amount. The term "alcoholic liver disease" (ALD) describes a condition that develops in the liver as an outcome of excessive alcohol use. ALD can be either acute or chronic, progressive or reversible, depending on the extent of damage and pathology[3]. The intake of alcohol is subjected as the main cause for developing alcoholic liver disease. The distinguishing feature of ALD's basic pathophysiology is macrovesicular steatosis, which can progress to alcoholic cirrhosis, alcoholic fibrosis, alcoholic steatohepatitis, and potentially hepatocellular cancer[4]. ALD is divided into four categories: cirrhosis, fibrosis, alcoholic fatty liver, and alcoholic hepatitis. ALD, or alcohol-related liver disease, is a worldwide health issue. An estimated 1.4% of people worldwide suffer from an alcohol use problem, while 1.3% of people suffer from alcohol dependency[5]. The pathophysiology of ALD is quite elaborated but majorly starts with prolonged and extreme alcohol consumption, which helps in activation of inflammatory signalling pathways inside the liver cells[6]. At the cellular level, alcohol metabolism generates oxidative stress and causes hepatocytes to undergo apoptosis. Removing alcohol results in the reversal of cellular damage to some extent. However, with continued or progressive exposure, apoptosis-induced release of intracellular contents results in heightened activation of Kupffer cells and mediates hepatocyte damage through the dysregulated release of pro-inflammatory cytokines and chemokines[7]. The inflammatory reaction also involves other parenchymal and non-parenchymal cells in the liver. As part of the so-called gut-liver axis, gut-derived bacterial pathogen-associated molecular pattern molecules are also important in the pathophysiology of ALD[8]. Germ-free mice are completely immune to the development of hepatic inflammation following alcohol consumption because alcohol-induced dysbiosis intensifies the severity of liver damage[8]. The specific molecular processes that contribute to liver injury as it progresses from simple fat buildup to more serious conditions like steatohepatitis or cirrhosis are not well understood. However, several factors such as alcohol metabolism, cell death, inflammasome signalling, and gut-derived toxins have been identified as playing significant roles in this progression. More recent research has also suggested that endoplasmic reticulum stress and specific receptors may contribute to the development of fibrosis in the liver[9]. Understanding these underlying mechanisms could help identify potential targets for therapeutic interventions. More recent research on the role of endoplasmic reticulum stress and receptors has also revealed evidence of fibrogenic pathways that act downstream of the canonical pathway that accelerates fibrosis in ALD[10]. Herbal compounds, natural compounds, or Phytochemical compounds have a variety of

active components that provide many opportunities and possibilities for drug discovery and development. Linoleic acid is a non-toxic product, and research has shown that regular in-take of linoleic acid can help in reducing the occurrence of Alcoholic liver disease[11]. Linoleic acid- Linoleic acid belongs to polyunsaturated fatty acid that's found in plant oils. Linoleic acid is an essential fatty acid required in human and nutrition. It is classified as an n-6 polyunsaturated fatty acid and has 18 carbons[12]. Linoleic acid is widely present in mycelia [13] of various mushrooms like *Hieracium Erinaceus*, *Pleurotus ostreatus*, *Ganoderma lucidum*, *Agaricus Bisporus* and can also be derived from vegetable oils, nuts, seeds, meat and eggs[14]. The IUPAC name of linoleic acid is (9Z,12Z)-octadeca-9,12-dienoic acid[15]. The molecular formula of linoleic acid is $C_{18}H_{32}O_2$ and its molecular weight is 280.4 g/mol[15]. Also, it is well known for displaying a wide variety of organic biological functions counting its anti-inflammatory, anti-cancer and anti-bacterial effects[16]. It contains anti-cancer properties and also plays a role in oxidative metabolism. As linoleic acid contains a variety of phytochemical substances the phytochemistry of linoleic acid has significant health benefits [17]. Due to its efficient and highly targeted control, human utilizes linoleic acid a potential curative agent for the preventing and treating ALD. Therefore, linoleic acid has been regarded as a combination of interest in the field of drug discovery as well as development[18].

However, the molecular mechanism of linoleic acid and phenotypic mutations of related cells has not been systematically known [19]. Linoleic acid can be esterified with glycerol[19]; it is obtained by the hydrolysis of natural fat as the corresponding glyceride. Linoleic acid contains two cis double bonds in the cis-9, cis-12 position. The double bonds are separated by 3 methylene (-CH₂-) units[20]. Based on the presence of greater than one double bond, note that linoleic acid is classified as a polyunsaturated fatty acid (PUFA). Physically, linoleic acid is a liquid, has a faint odour, and has a melting point of -5°C[21]. Due to its non-uniform molecular shape and the separation of the two double bonds by at least 3 (-CH₂-) units, linoleic acid is soluble in organic solvents and water. Linoleic acid is oxidized through enzymatic and nonenzymatic mechanism[22].

Biologically, linoleic acid will orient itself in cell membranes with approximately one-third of its length remaining in the hydrophilic environment and two-thirds remaining in the fatty acid portion[23]. The molecular-scale physical and functional characteristics of linoleic acid will [24]. Furthermore, this understanding can also be used to infer how dietary [25]. Therefore, understanding the structure can help you learn more about how linoleic acid affects your health. As a result of its effectiveness and flexibility for various purposes, as well as its safety in human use linoleic acid has attracted attention as a potential medicinal agent for the treating various ailments. Also, the benefit of targeted calculation methods for targeting and predicting drugs and potential alternatives has become an important method. These methods fasten up the procedure of drug discovery and development, also it is effective and save time and effort. For this reason, we evaluated the pharmacological benefits of Linoleic acid by using network pharmacology. First, we checked the TCMSP server. TCMSP was used to analysed the biological properties of Linoleic acid. Other possible and targeted genes were identified and evaluated by analysis of chemical and genetic interactions. These potential genetic targets were subject to nutritional analysis (GO) and (KEGG) and then cellular fishing (figure 1). Finally, the linoleic acid drug relationship network was used to explain the potential goals and method.

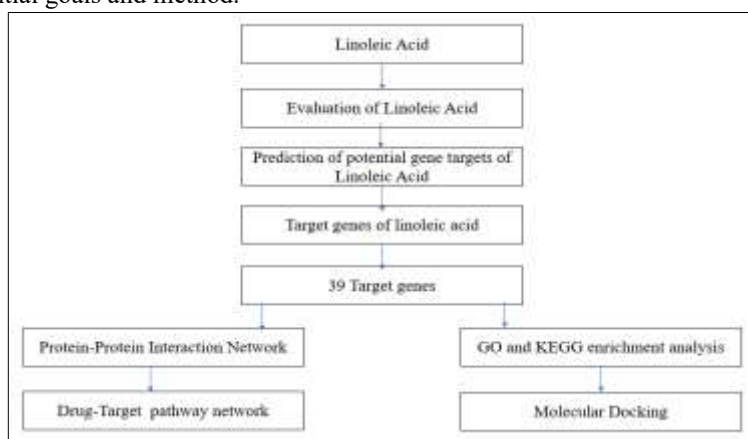


Figure 1 The flow of bioinformatics analysis of linoleic acid includes target gene prediction, ADME evaluation, GO enrichment analysis, KEGG enrichment analysis, the construction of protein-protein interaction network, the construction of the drug-target-pathway network, and molecular docking.

MATERIAL AND METHODS

2.1 OBTAINING CHEMICAL STRUCTURE FROM PubChem DATABASE

The chemical structure of the molecule (Linoleic acid) has been downloaded from PubChem database (<https://pubchem.ncbi.nlm.nih.gov/>)[26].

2.2 Pharmacokinetics testing by TCMSP

TCMSP represents the Chinese traditional medicine system (<http://lsp.nwu.edu.cn/tcmsp.php>), is a unique system of Chinese herbal / phytochemical medicine that captures the relationship between drugs, targets, and disease[27]. The site contains a drug-linked drug network, targeted and targeted drug networks and pharmacokinetics structures of natural compounds such as drug parallel, intestinal epithelial access, bioavailability, blood-brain barrier[28]. Consequently, the TCMSP database was used to “search” and “assess” the pharmacokinetic properties of linoleic acid in our investigation.

2.3 Identification of genes by the Comparative Toxicogenomic Database (CTD).

Comparative toxicogenomic (<http://ctdbase.org/>) helps in knowing relationship of drugs, genes and diseases[29]. It also provides valuable information on genetically related genes, genetic interactions, and chemical phenotype. Consequently, we predicted linoleic acid target genes using this database. As potential target genes, genes with interaction ≥ 1 are chosen[30].

2.4 Construction of a protein and protein network

It is an open-access bioinformatics tool that provides comprehensive information on protein–protein interactions (PPIs)[31]. It offers genetic and protein research resources and serves as a web platform for well-known and highly predicted PPIs. STRING enables system-level analysis of interaction networks offering insights into the structural, evolutionary, and functional features of proteins. In the context of alcoholic liver disease, such networks are particularly valuable for identifying linoleic acid binding proteins and understanding their roles in disease-associated cellular processes [32]. A total 38 targets of linoleic acid were uploaded to the STRING database, with the species set to Homo sapiens. The protein–protein interaction network was generated, and results were imported into Cytoscape for better visualization and analysis. STRING links even non-interacting proteins, such as inhibitors and activators within the same pathway[33, 34]

2.5 Gene function and pathway enrichment analysis by using Web Gestalt tool-

Web Gestalt stands for (WEB-based Gene Set Analysis Toolkit) (<http://www.webgestalt.org/option.php>) is an advanced web statistics tool which contains knowledge of genetic function and method enrichment analysis we will be using GO and KEGG analysis[35].

GO stands for gene ontology - a widely used method that helps to identify a group of genes that use a genetic classification system, 'in this gene depends on the functional attributes[36] KEGG is a source of data to understand the functions of high-level and biological systems, such as cells, organisms, and ecosystems, using genomic and molecular data[37, 38]. Thus, we are using the GO and KEGG databases for enrichment analysis after entering potential genes of target into the Webgestalt server.

2.6 Chemical- intended - pathway network construction-

Cytoscape is an open-source software platform designed for visualizing and integrating biomolecular interaction networks with high-throughput data and other molecular attributes. It allows the incorporation of metabolites such as linoleic acid into physiological and functional networks, thereby enabling the identification of key pathways and molecular interactions relevant to disease mechanisms. Further for better understandings we visualized the complex targets and their interaction between linoleic acid targets and pathways by visualizing them on Cytoscape.

2.7 The compound targets MOLECULAR DOCKING

To perform molecular docking studies, the chemical structure and molecular formula of the bioactive compound linoleic acid were first retrieved from the Comparative Toxicogenomic Database (CTD) in mol2 format. Subsequently, the three-dimensional crystallographic structures of the target proteins were obtained from the Protein Data Bank (PDB) (<https://www.rcsb.org/>) and saved in PDB format. Using PyMOL, all heteroatoms, including water molecules and co-crystallized ligands, were removed to prepare the receptor structures for docking.

In this study, molecular docking was performed using FDA-approved drugs for comparison purposes. Among the tested compounds, linoleic acid exhibited favourable docking interactions. The chemical structure of linoleic acid and reference ligands (oleic acid, myristic acid, and metformin) were obtained in mol2 format, while the crystal structure of the Peroxisome Proliferator-Activated Receptor Alpha (PPARA) protein (PDB ID: 2ZNN) [39] was retrieved from the Protein Data Bank (<https://www.rcsb.org/>) in PDB format. Solvent molecules and co-crystallized ligands were removed using PyMOL. Protein and ligand preparation, including hydrogen addition, charge assignment, torsional flexibility definition, and file conversion to PDBQT format, were performed using AutoDock Tools. Molecular docking was carried out using AutoDock, with the receptor treated as a rigid macromolecule and docking performed under the Lamarckian Genetic Algorithm (GA). The docked complexes were ranked based on binding energy, and the lowest-energy conformations were selected for further analysis. Docking poses and protein–ligand interactions were visualized in PyMOL, while two-dimensional interaction diagrams were generated using the Proteins Plus server (<https://proteins.plus/>) for generating 2D images.

2.8 Molecular dynamics simulation-

The simulation was performed to evaluate the protein–ligand complex's structural stability, conformational changes, and interaction dynamics of the protein–ligand complex under physiological conditions. The molecular dynamics workflow included various system preparation, energy minimization, equilibration, and a production run[40]. A 500 ns simulation was carried out using GROMACS 2021 to investigate the dynamic stability of the protein–ligand complex. Following the simulation, detailed analyses such as RMSD, RMSF, SASA, radius of gyration (Rg), free energy landscape (FEL), hydrogen bonding interactions, principal component analysis (PCA), and MM/PBSA were performed. These results provided insights into the structural changes, flexibility, and overall stability of the 2ZNN–linoleic acid complex[41].

Molecular Dynamics Trajectory Analysis

All trajectory analyses were performed using the built-in tools of **GROMACS**. The structural stability and dynamic behavior of the protein–ligand complex were evaluated over a 500 ns simulation period[42].

The root mean square deviation (RMSD) was calculated to monitor structural deviations of the complex throughout the simulation using standard analysis utilities. RMSD values were obtained as a function of simulation time, where time (ns) was plotted along the x-axis and deviation (nm) along the y-axis. The solvent accessible surface area (SASA) was computed to estimate the surface area of the protein–ligand complex exposed to the solvent. SASA calculations were carried out along the simulation trajectory to assess changes in solvent exposure over time.

The root mean square fluctuation (RMSF) was determined to quantify the flexibility of individual residues within the protein structure. RMSF values were calculated by measuring the average positional deviations of atoms from their mean coordinates during the simulation. The radius of gyration (Rg) was analyzed to evaluate the overall compactness of the protein–ligand complex. Rg values were computed as the mass-weighted root mean square distance of atoms from the center of mass of the system[42].

Principal Component Analysis and Free Energy Landscape

Principal component analysis (PCA) was performed to investigate large-scale collective motions of the protein during the molecular dynamics simulation. The first two principal components (PC1 and PC2) were extracted to represent the dominant motions of the system. Each point represents a simulation frame coloured according to time evolution (black → yellow), as indicated by the colour scale. PC1 and PC2 account for 76.06 % and 23.94 % of the total atomic motion, respectively, capturing nearly all essential conformational variance. The trajectory distribution shows an initial dispersion during the early phase (0–200 ns), followed by gradual convergence toward a single, dominant conformational basin after ~400 ns, indicating that the complex achieves structural equilibrium. The free energy landscape (FEL) was generated to explore the conformational space and thermodynamic stability of the system. FEL was constructed by projecting the trajectory onto selected reaction coordinates, specifically RMSD and radius of gyration (Rg)[43].

3. RESULTS

3.1 Molecular structural formula and pharmacokinetics of linoleic acid-

For obtaining the chemical structure of Linoleic acid and formula PubChem database was used $C_{18}H_{32}O_2$ is the molecular formula and (figure-2) showing the molecular structure of linoleic acid whereas the property of linoleic acid can be observed in table 1.



Figure -2 molecular structural of Linoleic acid (PubChem CID: 5280450)

Table -1 linoleic acid property from PubChem

Property Name	Property Value	Reference
Molecular Weight	280.4 g/mol	[44]
XLogP3	6.8	[44]
Hydrogen Bond Donor	1	[44]
Hydrogen Bond Acceptor Count	2	[44]
Rotatable Bond Count	14	[44]
Exact Mass	1	[44]

3.2 Pharmacokinetic characteristics of Linoleic acid evaluated from ADMET lab-MW: molecular weight; logP: lipophilicity coefficient (0- 3); BBB: blood brain barrier penetration; CL: clearance (>15mg/ml);

Table-2 ADMET properties of linoleic acid

Molecular Weight	Blood Brain Barrier Penetration	CL	LogP
280.24 Contain hydrogen atoms. Optimal:100~60	0.196	3.327	6.652

According to the evaluation, Linoleic acid is a nontoxic and has no carcinogenic properties, however it is a skin sensitizer, causes eye irritation, and has respiratory toxicity which needs to be overcome table-2.

3.3. Gene target prediction

Potential targets genes related to Linoleic acid were obtained through CTD database. In total 85 genes were retrieved out of which we choose only those genes whose interactions was more than 1. There were in total genes which we got whose interaction was above 1. These targeted genes were saved in Ms-excel for further analysis.

We downloaded an MS-Excel file which was containing all the 85 genes out of which we only selected those genes whose interaction was more than 1 out of 85 genes 39 genes were having the interaction which is 1 we opt out these 39genes and select those gene whose interactions is more than one.

3.4 PPI-Network by using STRING database-

Network studies help in prediction of different pathways related and effect of chemical on their interaction. To obtain the protein interaction and network relationship, all of the targets of linoleic acid were entered into the STRING database, and Homo sapiens was selected as the organism. The data were then imported into Cytoscape for visualisation after the free nodes were eliminated. (Figure-3) showing the network, the colour of nodes in circle is according to the degree value i.e., more the degree, darker is node colour. There are 38 nodes and 299 edges in the diagram. Calculated via mathematical analyser of network plugged into Cytoscape, average node degree 15.7. The top ten genes were extracted on the basis of degree method, closeness and centrality.

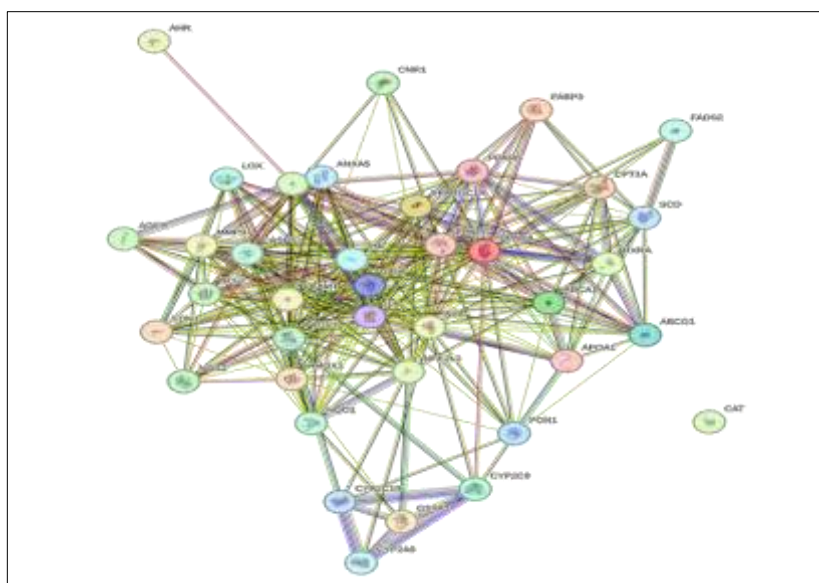


Fig-3 PPI network generated by STRING database illustrating number of nodes:38, number of edges: 299, number of degrees: 15.7

3.5 Target network of top 10 genes- by using cytoscape

The protein interaction network was examined when the material was exported into Cytoscape (figure 4) . Hub proteins were identified based on interaction degree, and bottleneck nodes were determined using the CytoHubba plugin. The highest-ranking proteins with the most interactions were chosen. Additionally, figure-4 a drug–target–pathway network was built to show the connections between linoleic acid, its targets, and related pathways. Topological interaction of top genes on the basis of degree method , Betweenness and Closeness method was done by using bottleneck genes table-3.

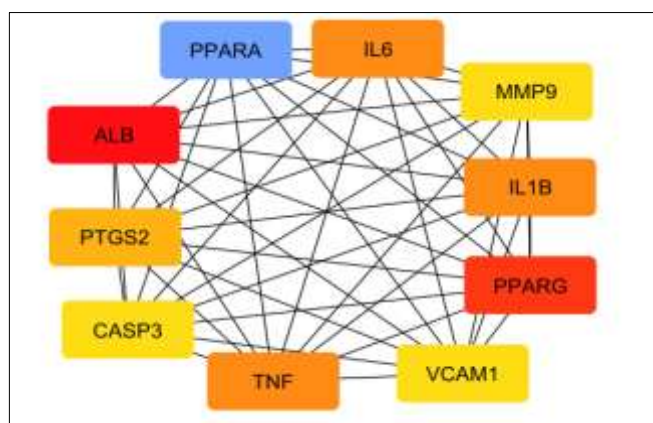


Fig- 4 showing the visual representation of top ten targeted genes by using cytoscape tool

Table: 3 Topological interaction of Top 10 on various topologies / methods

Rank	Name	Score	Rank	Name	Score	Rank	Name	Score
1	ALB	32	1	ALB	165.2108	1	ALB	34
2	PPARA	31	2	PPARA	94.66712	2	PPARA	33.5
3	PPARG	28	3	PPARG	84.1021	3	PPARG	32
4	TNF	27	4	TNF	78.46813	4	TNF	31.5
4	IL6	27	5	IL6	60.22006	4	IL6	31.5
4	IL1B	27	6	IL1B	34.0445	4	IL1B	31.5
7	PTGS2	25	6	PTGS2	34.0445	7	PTGS2	30.5
8	VCAM1	21	6	VCAM1	34.0445	8	VCAM1	28.5
8	MMP9	21	9	MMP9	27.66226	8	MMP9	28.5
8	CASP3	21	10	CASP3	27.37503	8	CASP3	28.5

(3a) Topological interaction of Top 10 ranked by Degree method

(3b) Topological interaction of Top 10 ranked by Betweenness method

(3c) Topological interaction of Top 10 ranked by Closeness method

3.6 Enrichment Analysis by using Webgestalt-

Then further, GO enrichment analysis of these 39 genes was performed by using web gestalt tool. GO enrichment analysis showed that most of all potential genes were involved in biological process (BP), cellular component (CC) and molecular function (MF) (figure-5).

Biological process enrichment analysis (BP) has (38/39) participating in all the biological process categories, metabolic process (37/39), response to stimulus (37/39), biological regulation (32/39), multicellular organismal process (30/39), cell communication (28/39), cellular component organization (28/39), developmental process (28/39), localization (27/39), cell proliferation (20/39) multi-organism process (18/39), reproduction (10/39), growth (7/39), unclassified (0/39).

Cellular component enrichment analysis (CC) has(38 /39) genes participating in all cellular component process, membrane(22/39), membrane enclosed lumen(21/39), endomembrane system(20 /39), nucleus(17/39), protein containing complex(17 /39), cytosol(16 /39), endoplasmic reticulum(16/39), extracellular space(15/39), vesicle(15/39), Golgi apparatus(6/39), mitochondrion(6/39), cell projection(5/39), chromosome(5 /39), endosome(4 /39), cytoskeleton(44 /39), extracellular matrix(4 /39), envelope(44/39), vacuole(2 /39), microbody(2/39), ribosome(1/39), unclassified (0/39).

Molecular function enrichment analysis(MF) has(38/39) genes participating in all Molecular function categories, protein binding(35/39), ion binding(32/39), nucleic acid binding(12/39), lipid binding (11/39), hydrolase activity (8/39), molecular transducer activity (7/39), molecular transporter activity (7/39), antioxidant activity (5/39), chromatin binding (4/39), nucleotide binding (4/39), enzyme regulator activity (3/39), oxygen binding (2/39), transferase activity (2/39), molecular adaptor activity (1/39), electron transfer activity (1/39), unclassified (1/39).

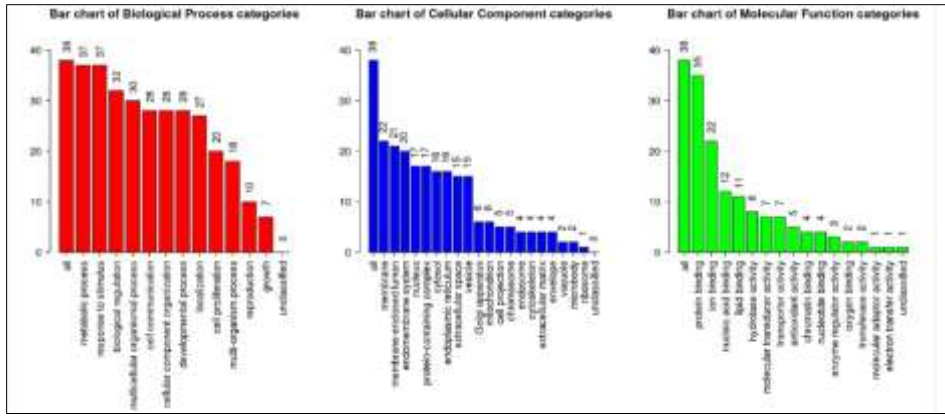


Fig-5 showing the bar graph representation of Biological process categories, cellular component categories, molecular function categories

3.7 KEGG Analysis: using shinyGo

KEGG study of these potential genes enrichment was performed by web gestalt application. Enrichment analysis showed 38target genes were enriched with 20 pathways and Alcoholic liver disease (figure 6) was significantly related with the target gene PPARA.PPAR-α is a nuclear receptor that functions as a transcription factor and plays a vital role in regulating lipid metabolism, especially mitochondrial and peroxisomal fatty acid β-oxidation. Further enrichment plot network pathway is generated different pathways affected by linoleic acid and interacted with potential gene targets of linoleic acid

can be observed. A significant KEGG pathway diagram was also generated using ShinyGo KEGG of Alcoholic liver disease with genes highlighted in red (figure 7) This suggests possible effects of linoleic acid and its potential gene targets on Alcoholic liver disease.

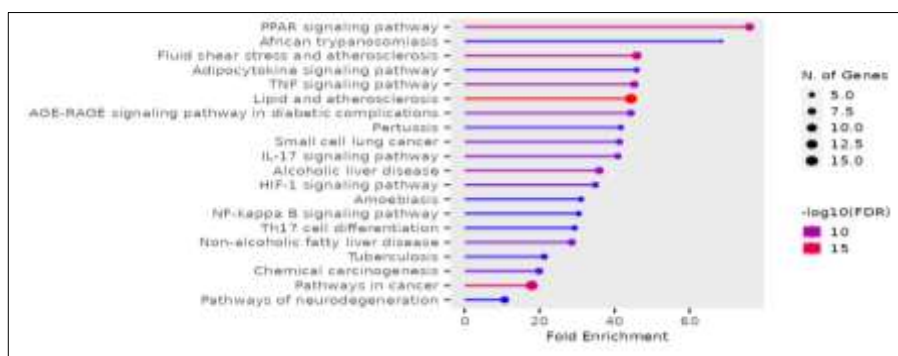


Fig-6 representation of 38 targeted genes enriched with alcoholic liver disease and 20 other pathways

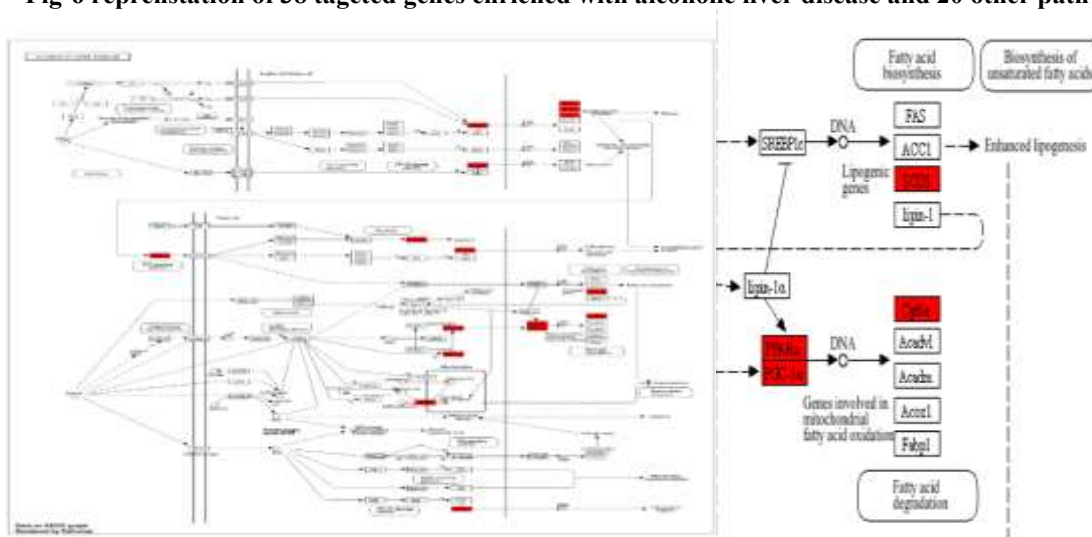
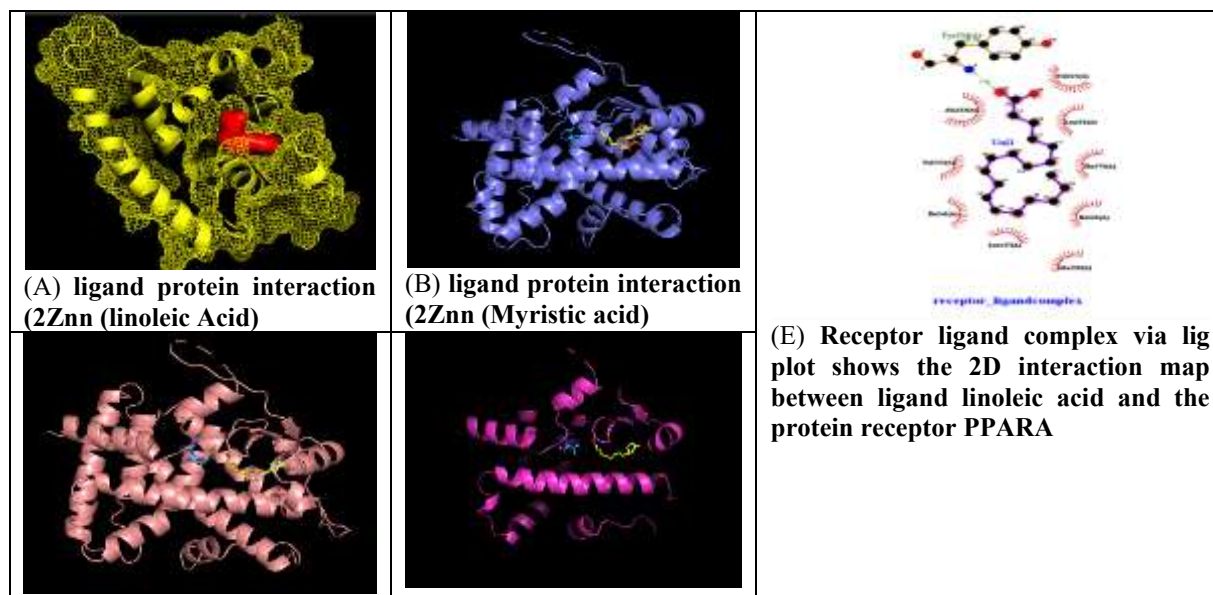


Figure 7-showing that PPARA is showing effectivity in treatment of Alcoholic Liver Disease

3.8 Molecular Docking

In cases where binding enthalpy of ligand & the receptor is lower indicating spatial stability, the probability of interaction is greater. In recent times there is no specified standardization for target bind and visualization of active molecules. The docking of linoleic acid was performed with 2Znn which the PPARA coding protein which plays an important role in lipid metabolism and alcohol induced hepatic injury. The docking results revealed protein 2Znn with ligand linoleic acid exhibited the -6.0kcal/mol affinity, which results that linoleic acid has the potential of being a drug on alcoholic liver disease. The docking complex demonstrated key hydrophobic and hydrogen bond interactions within the active binding pocket of the receptor, contributing to the overall binding stability.



(C) ligand protein interaction (2Znn (Oleic acid))	(D) ligand protein interaction (2Znn (Metformin))	
--	---	--

Figure 8 (A) ligand protein interaction (2Znn (linoleic Acid) in surface model, Figure8(B) ligand protein interaction (2Znn (Myristic acid) in surface model, Figure 8(C) ligand protein interaction (2Znn (Oleic acid) in surface model, Figure8 (D) ligand protein interaction (2Znn (Metformin) in surface model. Figure 8(E) Receptor ligand complex via lig plot shows the 2D interaction map between ligand linoleic acid and the protein receptor PPARA

The docking of other three FDA approved drugs which are oleic acid, myristic acid, metformin has also been performed. The molecular docking of FDA approved drugs OLEIC_ACID, MYRISTIC_ACID, METFORMIN clearly illustrates that linoleic acid is having better affinity as compared to FDA approved drugs Table- 4.

Table-4 binding affinity of FDA approved drugs with Linoleic acid

Compound	Affinity (Kcal/mol)
Linoleic acid	-6.0
Oleic acid	-5.7
Myristic acid	-5.4
Metformin	-5.1

3.9 MD simulation

To evaluate the molecular interactions between protein 2ZNN and the ligand linoleic acid, molecular dynamics (MD) simulations were performed as mentioned. The results indicated that, linoleic acid–protein complex remained stable with minimal structural deviation, confirming strong and consistent binding throughout the simulation period. These findings support the docking results and further highlight the potential of linoleic acid as a stable and effective molecule for targeting pathways involved in Alcoholic Liver Disease.

Stability Analysis (RMSD):

Initially during the course of MD simulation periods it represents that ligand is relatively stable within the binding pocket. The structure is mostly static or undergoing only minor, expected thermal fluctuations (vibrations),(figure-9) This indicates a bound state after wards the due to rapid conformational changes of tagert the fluctualltion is noticed. Lastly the ligand may have quickly left and then partially returned to a less stable configuration before another unbinding event overall the RMSD support the transient changes in the simulation experiments

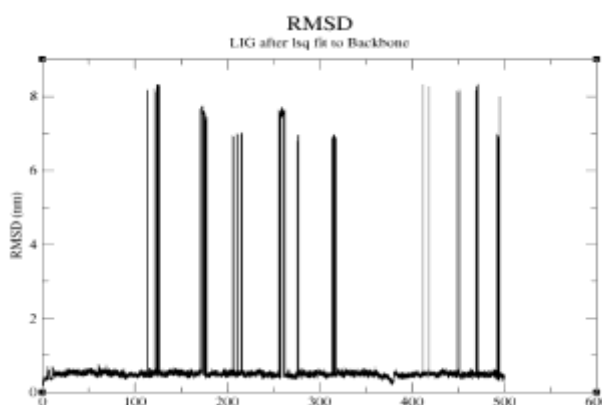


Figure-9 RMSD of protein in the complex

Compactness Analysis/Radius of Gyration (Rg)The graph demonstrates that the simulated structure is stable, well-folded, and compact over the simulated timescale further The Rg trace oscillates around a relatively constant average value of approximately 1.9 nm. (figure-10) This is the most crucial finding. It indicates that the molecule (likely a protein) maintains a stable, compact structure throughout the entire 500 ns simulation. There is no significant unfolding, aggregation, or large-scale swelling.

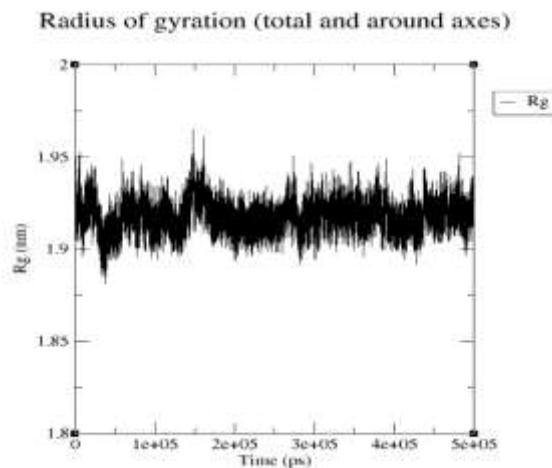


Figure-10 Radius of gyration Rg is showing structure stability and protein compactness

Flexibility Analysis (RMSF):

The sharp, high peaks (reaching up to 0.4 nm) indicate highly flexible regions of the molecule. These typically correspond to: Loop regions that connect secondary structure elements (figure-11) Terminal ends (N-terminus and C-terminus, visible as the spike near the end of the plot). Surface-exposed residues or regions involved in conformational changes (like domain movements).

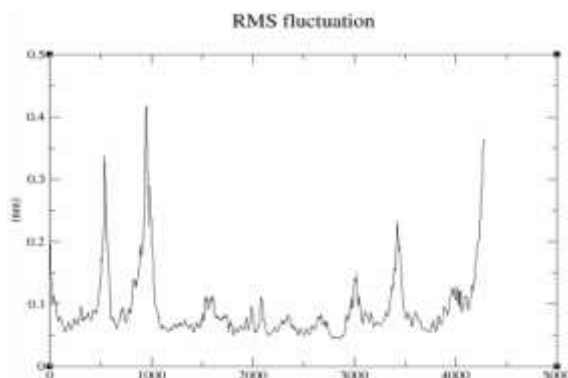


Figure -11 graph showing (RMSF) reveals that loop regions, terminal ends, and surface residues show higher flexibility (~0.4 nm), indicating dynamic but stable protein–ligand interaction

H bonds Analysis: graph plots the Number of Hydrogen Bonds against Time (ns) (nanoseconds). This graph provides a detailed time-resolved view of the persistence and stability of specific hydrogen bond(s) within the molecule or complex being studied. It is scientifically vital as H-bonds are the most common and crucial non-covalent interactions governing molecular structure, recognition, and function in biological systems (figure-12).

The plot shows a constantly fluctuating number of hydrogen bonds, most often ranging between 1 and 3 which is the expected behaviour for non-covalent interactions in a dynamic system like a protein-ligand complex or a protein structure. Hydrogen bonds are constantly being broken and reformed due to thermal energy and molecular motion. Notable The maximum number of H-bonds observed (around 3 or 4) represents the optimal interaction mode found during the simulation.

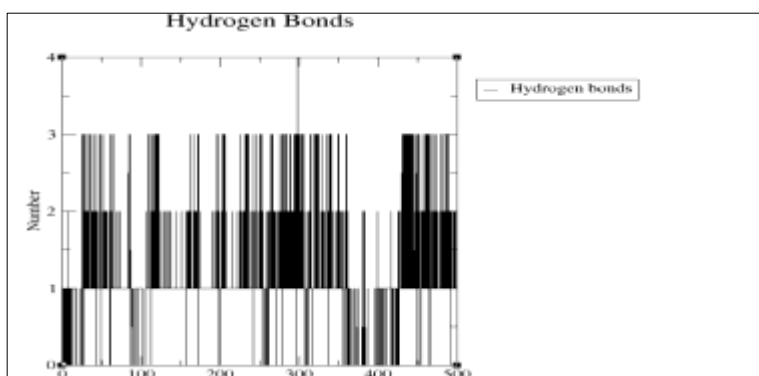


Figure 12- Radius of gyration graph remains stable around ~1.9 nm throughout 500 ns.

Analysis of SASA:

The image depicts a graph of the Solvent Accessible Surface (SAS) Area, measured in square nanometers (nm^2), plotted against time in picoseconds (ps). The rapid, irregular spikes indicate dynamic changes in the molecule's conformation, reflecting how its exposure to solvent varies as it moves or folds. Further SAS provides insights into how a molecule's shape and solvent exposure influence its stability and biological activity. The graph shows fluctuations in this area over time, with values ranging from approximately 15 to 25 nm^2 (Avg 20 nm^2). The rapid, irregular spikes indicate dynamic changes in the molecule's conformation, reflecting how its exposure to solvent varies as it moves or folds (figure-13). Finally protein-ligand complex remains stable with no major conformational changes (No significant drift) or unfolding occurred during the simulation.

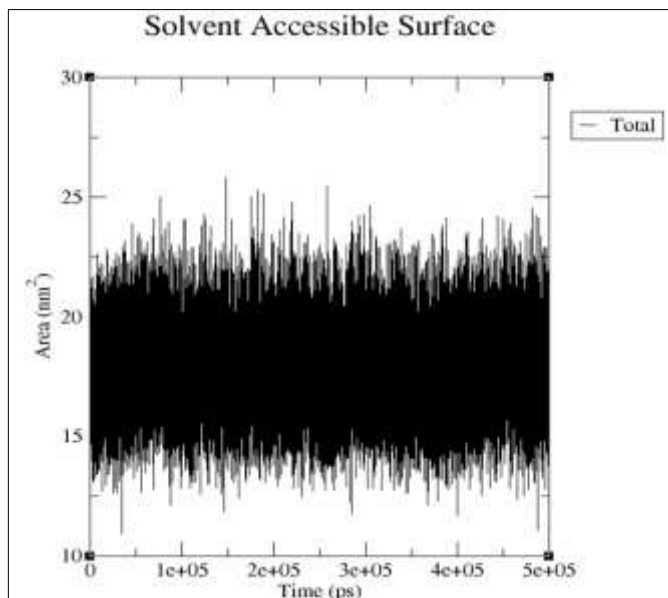


Figure 13- Measures solvent-accessible surface area over time

Principal Component Analysis:

Below given figure illustrates the exploration of different conformations of the 2H8H-Ponatinib and 2ZNN – linoleic acid complexes within the critical subspace.

Principal component analysis (PCA) of the wild-type (WT) 2ZNN–linoleic acid complex, projected along the first two principal components (PC1 and PC2), obtained from the 500 ns molecular dynamics trajectory. Each point represents a simulation frame coloured according to time evolution (black → yellow), as indicated by the colour scale. PC1 and PC2 account for 76.06 % and 23.94 % of the total atomic motion, respectively, capturing nearly all essential conformational variance. The trajectory distribution shows an initial dispersion during the early phase (0–200 ns), followed by gradual convergence toward a single, dominant conformational basin after ~400 ns, indicating that the complex achieves structural equilibrium (figure 14).

The continuous progression of the data points suggests smooth conformational transitions rather than abrupt state switching. Overall, the PCA reveals that linoleic acid binding stabilizes the protein structure while allowing limited collective flexibility of the binding domain—consistent with the favourable binding free energy ($\Delta G = -30.68 \text{ kJ mol}^{-1}$) determined by MM/PBSA analysis.

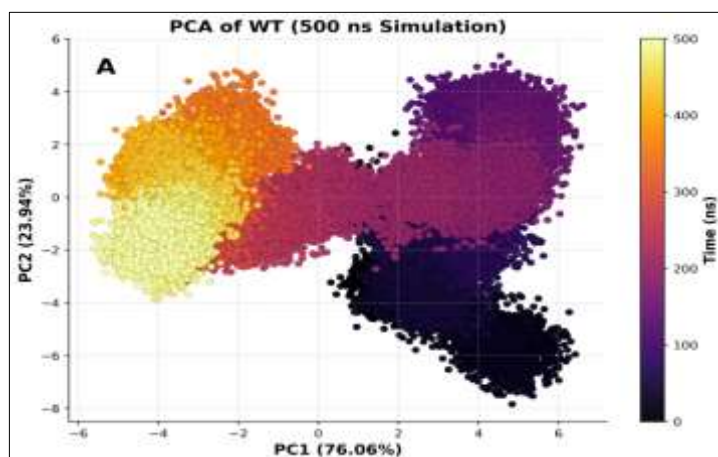


Figure 14- Principal Component Analysis (PCA) of the 2ZNN–Linoleic Acid Complex over 500 ns MD Simulation.

Gibbs Free Energy Landscape (FEL) Analysis:

The colour bar shows the free energy values in kJ/mol, with blue representing low free energy (stable states) and red representing high free energy (less stable states)

Free energy landscape (FEL) of the wild-type (WT) 2ZNN–linoleic acid complex plotted as a function of the first two principal components (PC1 and PC2), constructed from the 500 ns molecular dynamics trajectory. The colour gradient represents the relative Gibbs free energy (ΔG) distribution, (figure 15) where deep blue regions correspond to the lowest energy (most stable) conformations and red regions indicate higher-energy states. The landscape reveals a dominant global energy minimum surrounded by shallow local basins, suggesting that the system predominantly occupies a single, energetically favourable conformation with limited transitions between metastable states. This pattern reflects the structural convergence and thermodynamic stability of the complex, consistent with the PCA results and the favourable MM/PBSA binding free energy ($\Delta G = -30.68 \text{ kJ mol}^{-1}$). The presence of a broad, smooth basin further indicates that linoleic acid binding restricts large-scale conformational fluctuations, stabilizing the protein in a compact and energetically optimized configuration.

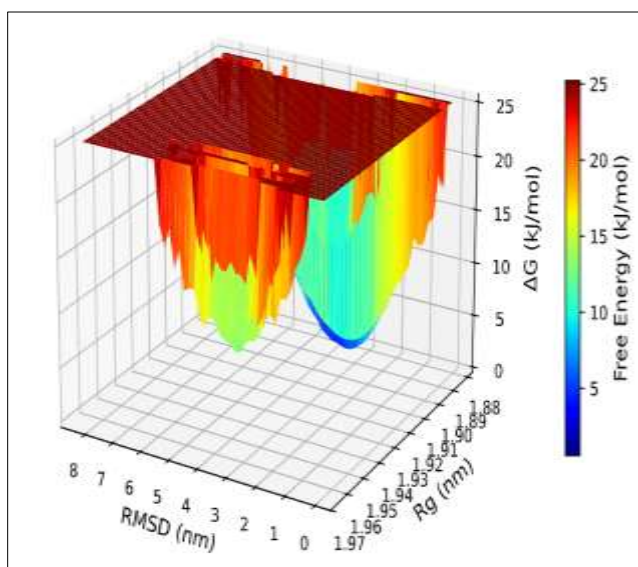


Figure 15- Free Energy Landscape (FEL) of the 2ZNN–Linoleic Acid Complex derived from 500 ns molecular dynamics simulation.

The prominent deep blue area in the foreground represents the global free energy minimum. Further this minimum is characterized by: Low RMSD (near 0-1 nm): The structure is very close to the reference structure and Low Rg (near 1.90-1.92 nm): The structure is compact. This is interpreted as the most stable, native (folded) state of the molecule. The low-energy regions (e.g., the shallow minimum around Rg 1.93 nm, RMSD 3 nm) are sub-minima or intermediate states. These represent temporarily stable, non-native conformations that the molecule can adopt before returning to the global minimum. Where as steep slopes separating the basins are energy barriers that must be overcome for the molecule to transition between states this reflects the overall stability of complex or transition needed much energy to alter the conformation Based on the provided graphs from the Molecular Dynamics (MD) simulation, the structural element or complex being studied exhibits mixed stability.

Estimation of Binding Free Energy (MM/PBSA):

The binding free energy of the 2ZNN–linoleic acid complex was computed using the Molecular Mechanics Poisson–Boltzmann Surface Area (MM/PBSA) method as implemented in gmxMMPBSA. Snapshots extracted from the 500 ns production trajectory were analyzed to estimate the enthalpic contribution to binding under implicit solvent conditions[4]

Table 5: Estimation of binding free energy

Energy Component	Average (kJ/mol)	SD	SEM	Contribution
Δ BOND	-0.00	0.00	0.00	Negligible (no strain)
Δ ANGLE	-0.00	0.00	0.00	Negligible (no strain)
Δ DIHED	-0.00	0.00	0.00	Negligible (no strain)
Δ VDWALS	-42.57	2.33	0.23	Strong favorable van der Waals attraction
Δ EEL	-2.50	3.38	0.34	Favorable electrostatic contribution
Δ EPB	+19.16	3.07	0.31	Unfavorable polar solvation penalty
Δ ENPOLAR	-4.77	0.14	0.01	Favorable hydrophobic/non-polar solvation

Energy Component	Average (kJ/mol)	SD	SEM	Contribution
ΔGGAS	-45.07	3.61	0.36	Net gas-phase attraction
ΔGSOLV	+14.39	3.03	0.30	Solvation penalty
ΔTOTAL	-30.68	3.21	0.32	Thermodynamically favorable

The calculated binding free energy ($\Delta G_{TOTAL} = -30.68$ kJ/mol) indicates a thermodynamically favourable and spontaneous association between the receptor and ligand. Energy decomposition analysis revealed that the interaction is primarily driven by non-polar van der Waals forces (-42.57 kJ/mol) and hydrophobic effects (-4.77 kJ/mol), while electrostatic contributions (-2.50 kJ/mol) provide additional stabilization. The major opposing factor, the polar solvation penalty ($+19.16$ kJ/mol), reflects the desolvation cost but does not outweigh the strong enthalpic attraction.

The total binding free energy ($\Delta G_{TOTAL} = -30.68$ kJ/mol) confirms that the interaction between linoleic acid and the 2ZNN receptor is spontaneous and energetically favourable.

Overall, the results demonstrate that hydrophobic interactions dominate the stabilization of the 2ZNN–linoleic acid complex, with negligible structural strain and sustained conformational rigidity in the binding region. These findings suggest that linoleic acid binds favourably within the hydrophobic pocket of 2ZNN, potentially contributing to the protein's functional modulation through stable, non-polar interactions.

Contribution of Major Energy Components to ΔG

Table 6- Contribution of major energy components to the binding free energy ΔG and their roles in ligand-protein binding

Interaction Type	Energy Component	Contribution (kJ/mol)	Percentage Total (%)	Role in Binding
Non-Polar	$\Delta VDWAAALS$ $\Delta ENPOLAR$	+ -47.34	~155%	Dominant favourable forces
Electrostatic	ΔEEL	-2.50	~8%	Secondary favourable term
Polar Solvation	ΔEPB	+19.16	-62%	Main unfavourable contribution
NetBinding Energy	$\Delta TOTAL$	-30.68	100%	Spontaneous complexation

CONCLUSION

Linoleic acid is having numerous pharmacological properties, according to our research. Simultaneously, we investigated that linoleic acid potential mechanism of action, which can be exploited to design more effective anti-inflammatory and anticancer medications. Our findings offer a fresh perspective on Linoleic acid research, development, and therapeutic application. These results suggest that linoleic acid interacts with multiple genes, proteins, and pathways to form an integrated pharmacological network, indicating its potential value in drug development and therapeutic applications. Limitations like skin sensitization, eye irritant respiratory toxicity, lesser oral bioavailability are barriers that has to be overcome in order to develop linoleic acid as a drug. Finally molecular docking about targets and Linoleic was done. Our data reflected that linoleic acid has profound biological activity and drug utilization. 38 gene targets were identified. The bioinformatics analysis and network analysis found that these target genes are closely related to each other. The results showed that linoleic acid can interact with various proteins and pathways such as Alcoholic Liver Disease also the Linoleic acid was compared to other FDA approved drugs which clearly shows that the binding affinity of FDA approved drugs for Alcoholic liver disease is better with Linoleic acid. Therefore, it can be used to form a systematic pharmacological network, which has good value in drug development and utilization to gain the structural stability after the MD simulation for 500 ns has been performed where it has been found that the ligand complex is showing the mixed behaviours and over all conformationally stable binding apart from that the The Rg value suggest the molecular compactness and stabilisation whereas RMS support that the core secondary structure are rigid and stable the high peaks are reflecting the flexibility at loop region of protein which is normal for a functional protein. Further SASA also provides insights of molecule's shape and solvent exposure influence its stability and biological activity. The overall core scaffold of the molecule itself is structurally stable and compact and interaction fluctuate but making it transient stable to support further for gaining deeper insight into the thermodynamic stability and conformational preferences observed in the PCA, the Free Energy Landscape (FEL) of the 2ZNN–linoleic acid complex was constructed using the first two principal components (PC1 and PC2) as reaction coordinates. While PCA primarily delineates the collective atomic motions throughout the simulation, FEL analysis provides the energetic perspective of these conformational states. The combined analysis enables correlation of the dominant structural fluctuations with their corresponding free energy basins, thereby offering a comprehensive view of the system's dynamic behaviour. The resulting FEL (Figure) reveals a single deep global minimum, corroborating the PCA findings that the complex undergoes smooth relaxation toward a stable equilibrium state without significant conformational switching. This thermodynamic profile supports the MM/PBSA results, confirming

that linoleic acid binding at with hydrophobic interaction drives the 2ZNN complex toward a low-energy, structurally stable conformation. Therefore, it can be used to form a systematic pharmacological network, which has good value in drug development and utilization.

Acknowledgement

We are thankful for Jaypee Institute of Information Technology NOIDA for all necessary support to conduct this study

REFERENCES

1. Younossi, Z.M., et al., The global burden of liver disease. *Clinical Gastroenterology and Hepatology*, 2023. **21**(8): p. 1978–1991.
2. Danpanichkul, P., et al., Global and regional burden of alcohol-associated liver disease and alcohol use disorder in the elderly. *JHEP Reports*, 2024. **6**(4): p. 101020.
3. Malnick, S.D., et al., Fatty liver disease-alcoholic and non-alcoholic: similar but different. *International Journal of Molecular Sciences*, 2022. **23**(24): p. 16226.
4. Ha, Y., I. Jeong, and T.H. Kim, Alcohol-related liver disease: an overview on pathophysiology, diagnosis and therapeutic perspectives. *Biomedicines*, 2022. **10**(10): p. 2530.
5. Subramanian, V., et al., Alcohol-associated liver disease: A review on its pathophysiology, diagnosis and drug therapy. *Toxicology reports*, 2021. **8**: p. 376–385.
6. Xiao, J., et al., Epidemiological realities of alcoholic liver disease: global burden, research trends, and therapeutic promise. *Gene expression*, 2020. **20**(2): p. 105.
7. Tang, S.-p., et al., Reactive oxygen species induce fatty liver and ischemia-reperfusion injury by promoting inflammation and cell death. *Frontiers in immunology*, 2022. **13**: p. 870239.
8. Cheng, Z., L. Yang, and H. Chu, The role of gut microbiota, exosomes, and their interaction in the pathogenesis of ALD. *Journal of Advanced Research*, 2024.
9. Ajoalabady, A., et al., Endoplasmic reticulum stress in liver diseases. *Hepatology*, 2023. **77**(2): p. 619–639.
10. Scarlata, G.G.M., et al., The Role of Cytokines in the Pathogenesis and Treatment of Alcoholic Liver Disease. *Diseases*, 2024. **12**(4): p. 69.
11. Whelan, J. and K. Fritsche, Linoleic acid. *Advances in nutrition*, 2013. **4**(3): p. 311–312.
12. Brenner, R.R. and R.O. Peluffo, Regulation of unsaturated fatty acids biosynthesis 1. Effect of unsaturated fatty acid of 18 carbons on the microsomal desaturation of linoleic acid into γ -linolenic acid. *Biochimica et Biophysica Acta (BBA)-Lipids and Lipid Metabolism*, 1969. **176**(3): p. 471–479.
13. Shaw, R., The occurrence of γ -linolenic acid in fungi. *Biochimica et Biophysica Acta (BBA)-Lipids and Lipid Metabolism*, 1965. **98**(2): p. 230–237.
14. Reyes, V., O. Martínez, and G. Hernández, National center for biotechnology information. *Plant Breeding. Universidad Autónoma Agraria Antonio Narro, Calzada Antonio Narro*, 1923.
15. Chen, Z., et al., Reassessment of the antioxidant activity of conjugated linoleic acids. *Journal of the American Oil Chemists' Society*, 1997. **74**: p. 749–753.
16. Aydin, R., Conjugated linoleic acid: chemical structure, sources and biological properties. *Turkish Journal of Veterinary & Animal Sciences*, 2005. **29**(2): p. 189–195.
17. Liavonchanka, A. and I. Feussner, Biochemistry of PUFA double bond isomerases producing conjugated linoleic acid. *ChemBioChem*, 2008. **9**(12): p. 1867–1872.
18. Ueno, S., et al., Polymorphism of linoleic acid (cis-9, cis-12-Octadecadienoic acid) and α -linolenic acid (cis-9, cis-12, cis-15-Octadecatrienoic acid). *Chemistry and Physics of Lipids*, 2000. **107**(2): p. 169–178.
19. Santoro, N., S. Caprio, and A.E. Feldstein, Oxidized metabolites of linoleic acid as biomarkers of liver injury in nonalcoholic steatohepatitis. *Clinical lipidology*, 2013. **8**(4): p. 411–418.
20. Fisher, C. and T.R. Scott, Food flavours: biology and chemistry. 2020: Royal Society of chemistry.
21. Zárate, R., et al., Significance of long chain polyunsaturated fatty acids in human health. *Clinical and translational medicine*, 2017. **6**: p. 1–19.
22. Zock, P.L. and M.B. Katan, Hydrogenation alternatives: effects of trans fatty acids and stearic acid versus linoleic acid on serum lipids and lipoproteins in humans. *Journal of lipid research*, 1992. **33**(3): p. 399–410.
23. Eigenschink, M., et al., A critical examination of the main premises of Traditional Chinese Medicine. *Wiener Klinische Wochenschrift*, 2020. **132**: p. 260–273.
24. Eigenschink, M., et al., Traditional Chinese medicine: A Bayesian network model of public awareness, usage determinants, and perception of scientific support in Austria. *medRxiv*, 2021: p. 2021.12. 24.21268331.
25. Li, S., et al., Lipidomics reveals serum lipid metabolism disorders in CTD-induced liver injury. *BMC Pharmacology and Toxicology*, 2024. **25**(1): p. 10.
26. Davis, A.P., et al., Comparative toxicogenomics database's 20th anniversary: update 2025. *Nucleic acids research*, 2025. **53**(D1): p. D1328–D1334.
27. Szklarczyk, D., et al., STRING v11: protein–protein association networks with increased coverage, supporting functional discovery in genome-wide experimental datasets. *Nucleic acids research*, 2019. **47**(D1): p. D607–D613.
28. Yu, H., et al., Annotation transfer between genomes: protein–protein interologs and protein–DNA regulogs. *Genome research*, 2004. **14**(6): p. 1107–1118.
29. Bajpai, A.K., et al., Systematic comparison of the protein-protein interaction databases from a user's perspective. *Journal of Biomedical Informatics*, 2020. **103**: p. 103380.

30. Szklarczyk, D., et al., The STRING database in 2017: quality-controlled protein–protein association networks, made broadly accessible. *Nucleic acids research*, 2016: p. gkw937.
31. Kanehisa, M., Kegg: Kyoto encyclopedia of genes and genomes. *Proc. Natl. Acad. Sci.*, 2001. **98**: p. 4569–4574.
32. Kanehisa, M., et al., KEGG: new perspectives on genomes, pathways, diseases and drugs. *Nucleic acids research*, 2017. **45**(D1): p. D353–D361.
33. Kanehisa, M., et al., KEGG for linking genomes to life and the environment. *Nucleic acids research*, 2007. **36**(suppl_1): p. D480–D484.
34. Mandal, S.K., et al., Targeting lipid-sensing nuclear receptors PPAR (α , γ , β/δ): HTVS and molecular docking/dynamics analysis of pharmacological ligands as potential pan-PPAR agonists. *Molecular Diversity*, 2024. **28**(3): p. 1423–1438.
35. Martin, R.L., et al., High-throughput structure-based drug design (HT-SBDD) using drug docking, fragment molecular orbital calculations, and molecular dynamic techniques. *High Performance Computing for Drug Discovery and Biomedicine*, 2023: p. 293–306.
36. Justino, D.M., D.R. Barreira, and D.G. Justino, analysis of residue interaction networks in molecular dynamics simulations. 2022.
37. Taghvaei, S. and L. Saremi, Molecular Dynamics Simulation and Essential Dynamics of Deleterious Proline 12 Alanine Single-Nucleotide Polymorphism in PPAR γ 2 Associated with Type 2 Diabetes, Cardiovascular Disease, and Nonalcoholic Fatty Liver Disease. *PPAR research*, 2022. **2022**(1): p. 3833668.
38. Roccatano, D., Principal component analysis of molecular dynamic trajectories: Concepts, Tools, and applications. *Wiley Interdisciplinary Reviews: Computational Molecular Science*, 2025. **15**(6): p. e70060.
39. Tripathi PK, Jain CK. Unravelling Phyto-Compound Therapeutics Against Colorectal Cancer: Targeting SRC proto-oncogene via Fibroblast Growth Factor Signalling Pathway -A Comprehensive Approach Integrating Omics Data Analysis, Network Pharmacology, Virtual Screening, and Molecular Dynamics. *Recent Adv Food Nutr Agric*. 2025;16(2):185-205. doi: 10.2174/012772574X294492240527081926. PMID: 38919088.